



Supplementary Information for

**Tonoplast-localized Ca<sup>2+</sup> pumps regulate Ca<sup>2+</sup> signals during pattern-triggered immunity in *Arabidopsis thaliana*.**

Richard Hilleary, Julio Paez-Valencia, Cullen Vens, Masatsugu Toyota, Michael Palmgren, Simon Gilroy

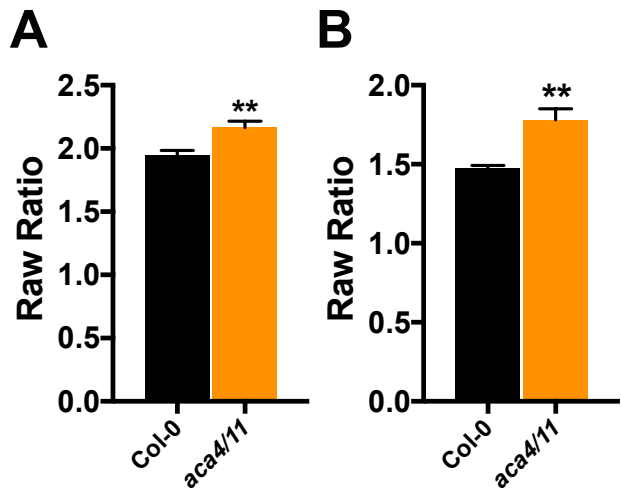
Simon Gilroy  
Email: sgilroy@wisc.edu

**This PDF file includes:**

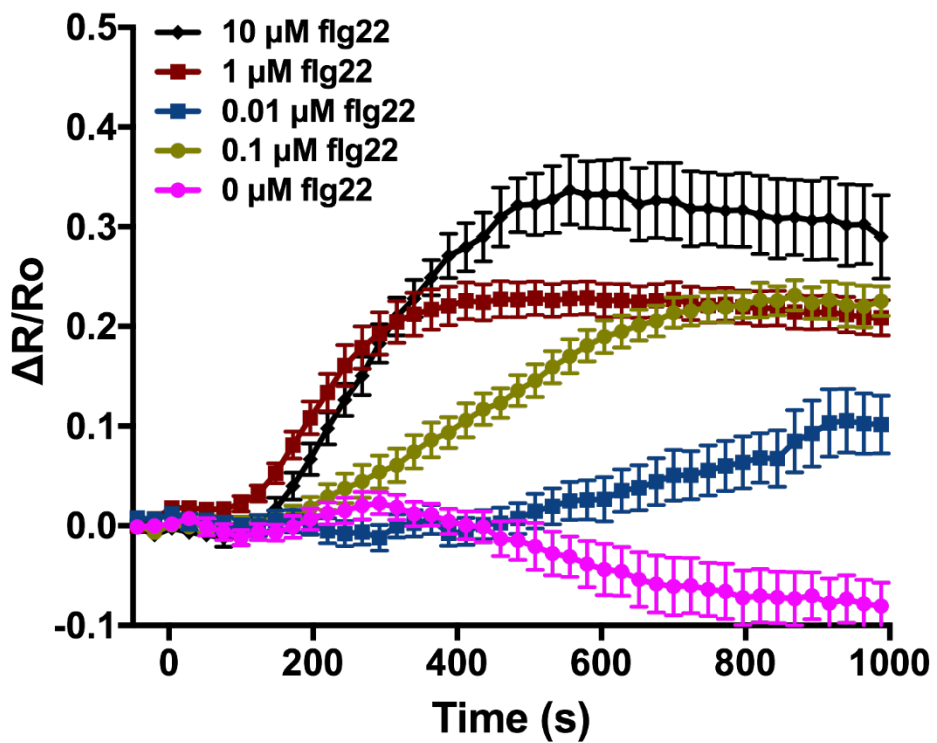
Figures S1 to S13  
Tables S1 to S2  
Legends for Movies S1 to S5

**Other supplementary materials for this manuscript include the following:**

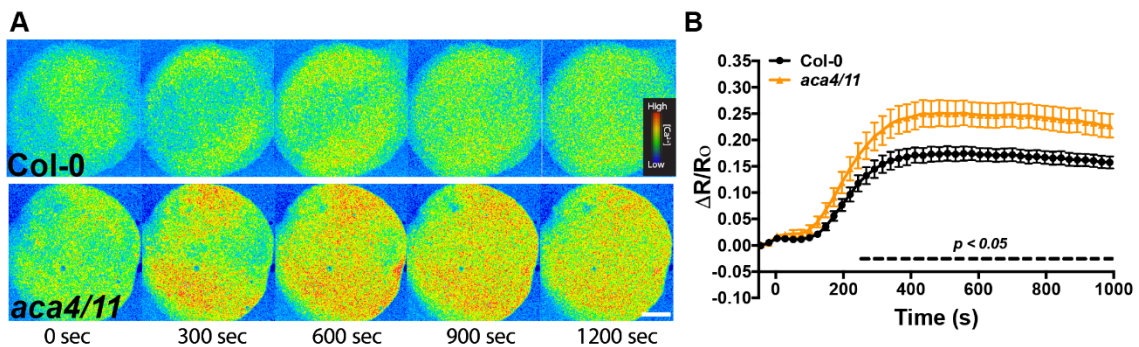
Movies S1 to S5



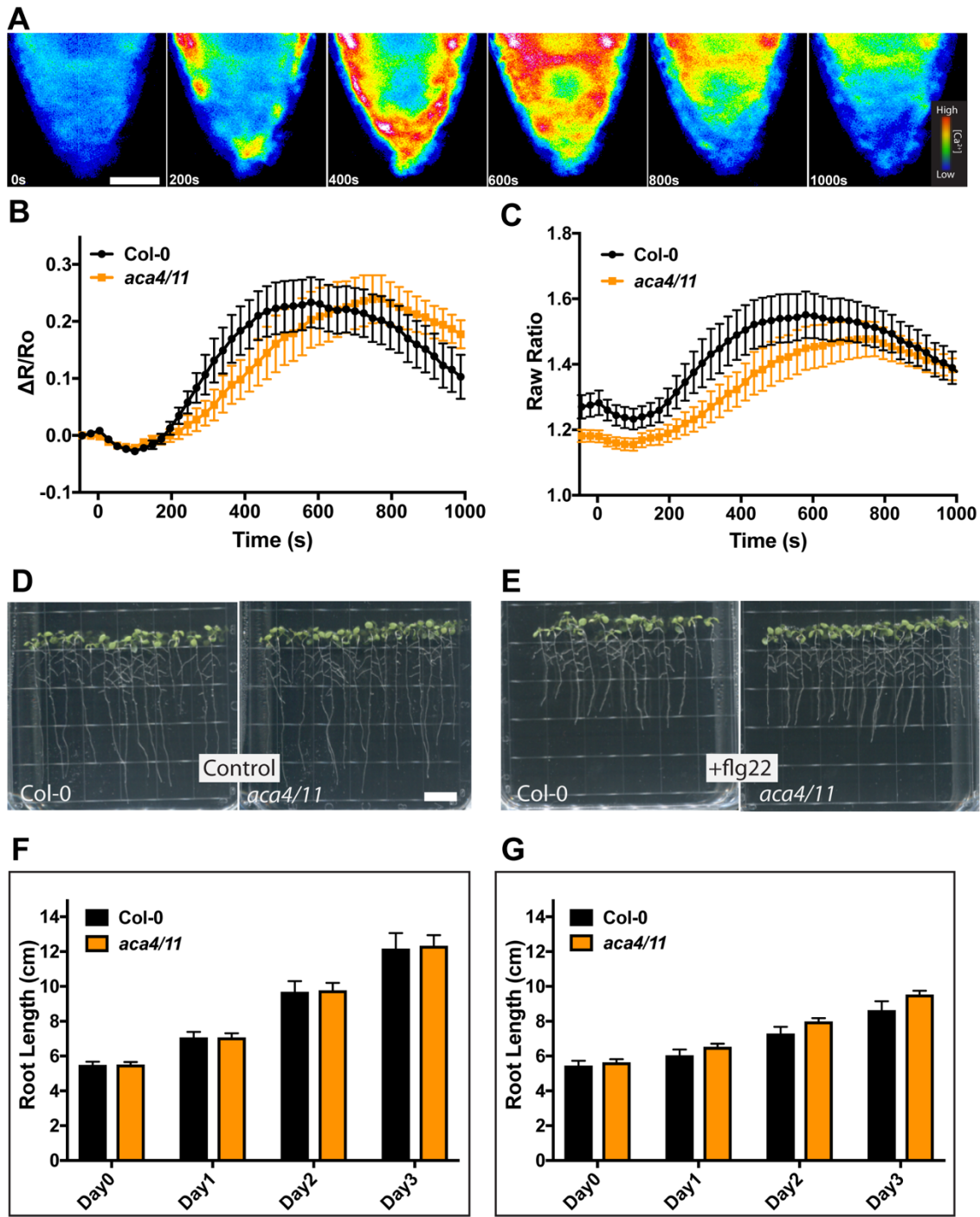
**Figure S1. Baseline FRET ratio values in Col-0 and *aca4/11* cotyledons.** Baseline raw FRET:CFP values were obtained from cotyledons of 10-day-old seedlings expressing YC-Nano65 that were (**A**) intact or had been (**B**) detached for 24 hours (mean  $\pm$  s.e.m., n = 8; Student's t-test, \*\*  $p < 0.01$ ). FRET values were obtained every 4 seconds and averaged over 15 minutes of imaging per replicate.



**Figure S2. Col-0 cotyledon responses to dilution series of flg22.** A dilution series of 0–10  $\mu\text{M}$  flg22 dissolved in  $\frac{1}{2}$  LS media was performed on Col-0 cotyledons to determine a concentration that elicited a strong response but was not saturating. Flg22 added at time = 0 sec. Data are presented as mean FRET  $\pm$  s.e.m.;  $n \geq 6$  for each concentration.

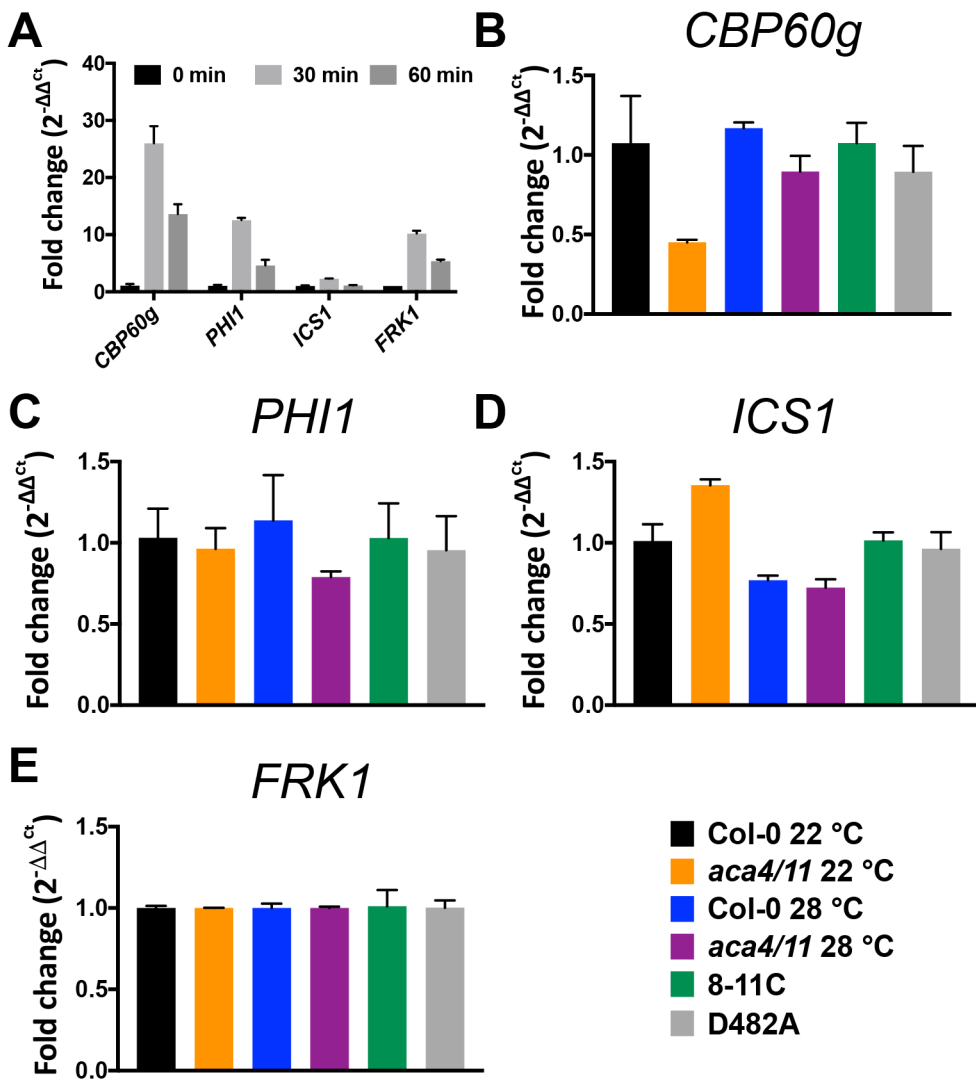


**Figure S3. *aca4/11* cotyledons exhibit an elevated  $\text{Ca}^{2+}$  signal in response to flg22.** (A) Time series FRET:CFP images of Col-0 and *aca4/11* cotyledons treated with 1  $\mu\text{M}$  flg22 at 0 sec. (B) Flg22-dependent  $\text{Ca}^{2+}$  signals are elevated in *aca4/11* when compared to wild type Col-0. Data presented as mean  $\Delta R/R_0 \pm \text{s.e.m.}$  ( $n \geq 15$ ).  $\Delta R$ , change in FRET:CFP;  $R_0$  FRET:CFP prior to treatment. Dashed line indicates time points showing significant differences in  $\Delta R/R_0$  values between wild type and *aca4/11* (Two-way ANOVA; Bonferroni-HSD;  $p < 0.05$ ).

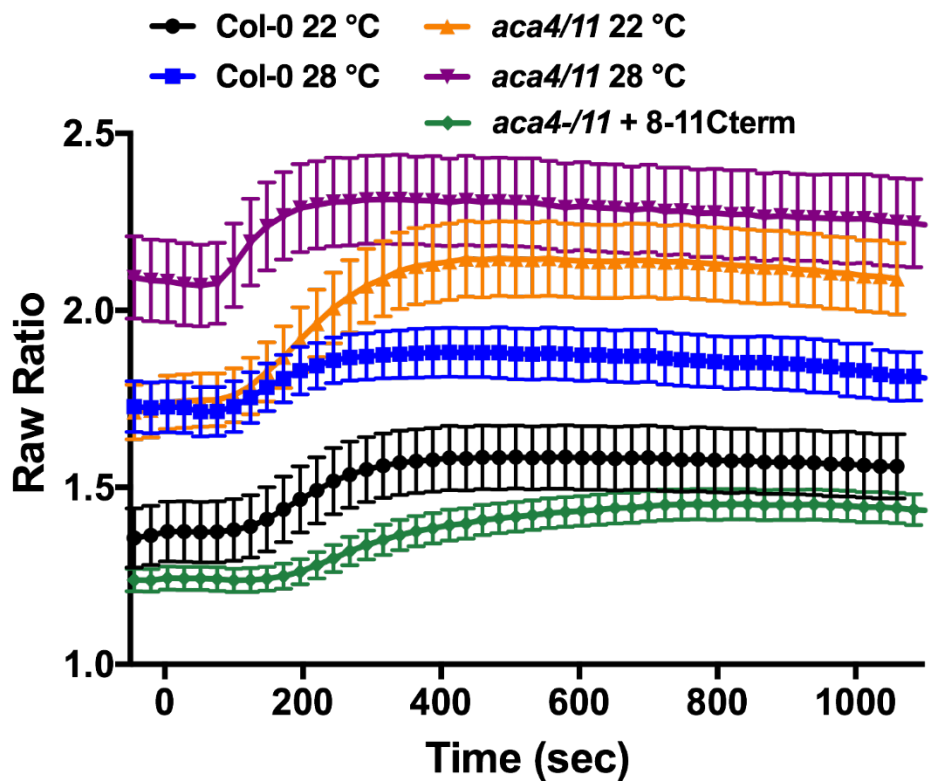


**Figure S4. Col-0 and *aca4/11* exhibit similar flg22-dependent phenotypes in roots.** flg22-dependent  $\text{Ca}^{2+}$  signals at the root tip and flg22-dependent growth inhibition are not significantly different between Col-0 and *aca4/11*. (A) Time series FRET images of Col-0 root tip after 1  $\mu\text{M}$  flg22 treatment at time = 0 sec. Representative images of  $n \geq 15$  separate experiments. Scale bar represents 25  $\mu\text{m}$ . FRET ratios (normalized YFP emission:CFP emission) are color-coded according to the inset scale. Normalized (B) and raw (C) quantitative FRET ratiometric data of Col-0 and *aca4/11* root tips after 1  $\mu\text{M}$  flg22

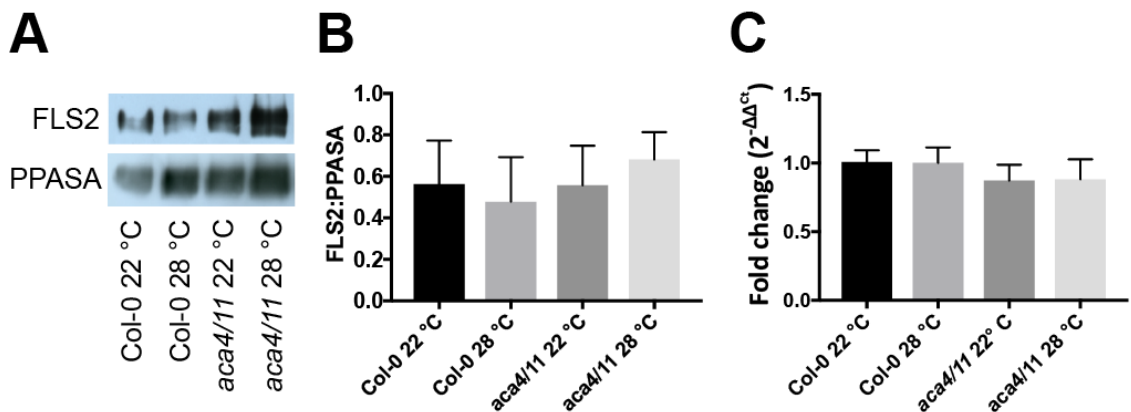
treatment. Data is displayed as mean  $\pm$  s.e.m.;  $n \geq 15$  biological replicates. Note: *aca4/11* Ca<sup>2+</sup> increase at the root tip appears slightly delayed, but there are no statistically significant differences between Col-0 and *aca4/11* at any time points (Two-way ANOVA; Tukey's HSD;  $p > 0.05$ ,  $n \geq 15$  replicates for each genotype). **(D and E)** Seedlings were germinated and grown on  $\frac{1}{2}$  LS solid media containing 10 mM sucrose, then transferred to control (**D**) plates (10 mM sucrose  $\frac{1}{2}$  LS) or plates containing 1  $\mu$ M flg22 (**E**). Scale bar represents 12 mm. **(F and G)** Root lengths were obtained for three days after transfer of seedlings to plates. Col-0 and *aca4/11* seedlings transferred to control plates (**F**) or flg22 plates (**G**) did not exhibit any significant differences in growth over three days (one-way ANOVA; Bonferroni HSD;  $p > 0.05$ ;  $n \geq 20$  replicates per genotype and treatment).



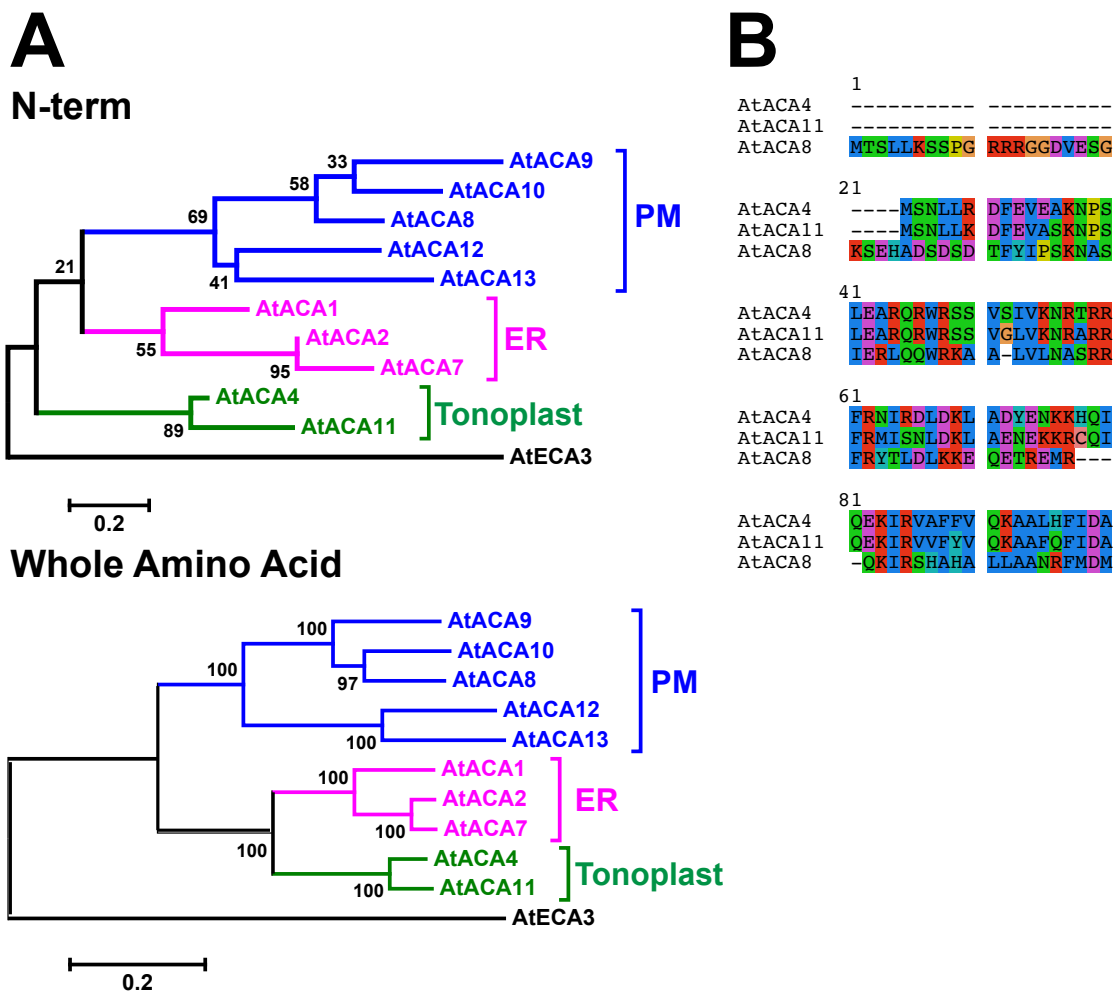
**Figure S5. Time-series of flg22-dependent transcriptional changes in Col-0, *aca4/11*, *aca4/11* + ACA8-11C, and *aca4/11* + D482A.** (A) Transcriptional responses in 10 day-old Col-0 seedlings treated with 1  $\mu$ M flg22 at 0 min. (B-E) fold-change in expression of *CBP60g*, *PHI1*, *ICS1* and *FRK1* at 0 min of flg22 treatment at 22 °C and 28 °C relative to Col-0 at 22 °C. Transcriptional activity for *aca4/11* + ACA8-11C and *aca4/11* + D482A were obtained from seedlings grown at 22 °C. Data represent mean  $\pm$  s.e.m. of 3 biological replicates. (B-E) No significant differences were detected (ANOVA  $p > 0.05$ ).



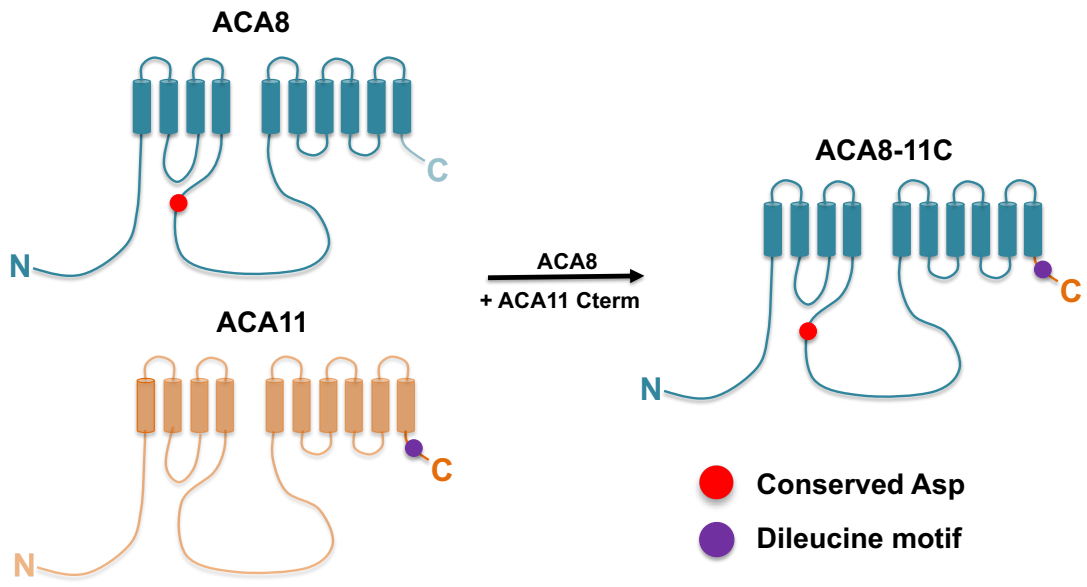
**Figure S6. FRET ratio value time series for cotyledons treated with flg22.** Time series of FRET ratio values without normalization are presented to show differences in baseline FRET values and response to 1  $\mu$ M flg22. Data represents mean  $\pm$  s.e.m. of  $n \geq 15$  biological replicates for each genotype/treatment. Data in 4D and E are taken from this timecourse. *aca4/11* + ACA8-11Cterm data was obtained from plants grown and imaged at 22 °C.



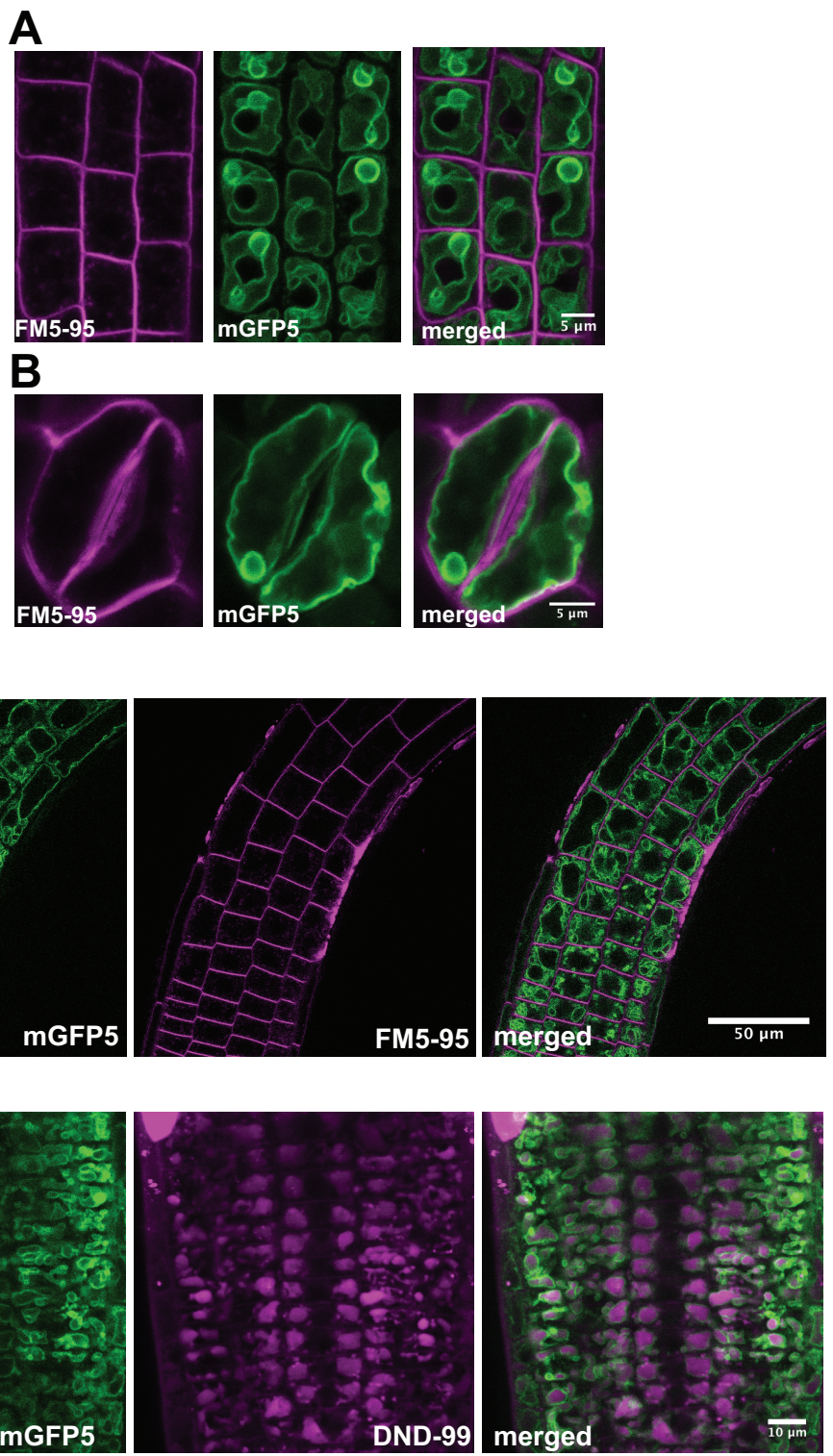
**Figure S7. FLS2 protein and transcript levels are similar between Col-0 and *aca4/11*.** Protein and transcript levels of FLS2 were assessed to determine if there were any significant differences between Col-0 and *aca4/11* or between seedlings grown at 22 °C or 28 °C. **(A)** Western blot of microsomal fractions showing levels of the FLS2 receptor and the vacuolar pyrophosphatase (PPASA; loading control). **(B)** The intensity of the bands were quantified by densitometry and the ratio of FLS2::PPASA from three independent western blots was obtained. No significant difference between genotypes or temperature treatments were detected (One-way ANOVA; Tukey's-HSD;  $p > 0.05$ ). Data represent mean ratio  $\pm$  s.e.m of 3 biological replicates **(C)** Transcript levels of *FLS2* as determined by qPCR show no significant differences between Col-0 and *aca4/11* or temperature treatments (One-way ANOVA; Tukey's HSD;  $p > 0.05$ ). Data represent mean  $\pm$  s.e.m. of 3 biological replicates.



**Figure S8. Phylogenetic tree of ACAs based on whole amino acid or N-terminal sequences.** (A) Neighbor joining trees for either N-terminal autoinhibitory domain or whole amino acid sequences of *Arabidopsis thaliana* ACA cluster based on subcellular localization. The ER-localized non-ACA pump ECA3 was used as an outgroup. All bootstrap values are shown to display the complete output of the analysis. (B) Alignment of the N-terminal autoinhibitory domain amino acid sequences of ACA4, ACA11, and ACA8.



**Figure S9. Structural features of ACA8 and ACA11.** The conserved aspartate residue is essential for the ATPase activity of the pump and is required to translocate  $\text{Ca}^{2+}$  against an electrochemical gradient. The C-terminal dileucine motif is required for vacuolar targeting. ACA8-11C is a C-terminal domain-swap between ACA8 and ACA11 incorporating the vacuolar targeting domain into the normally plasma membrane resident ACA8.



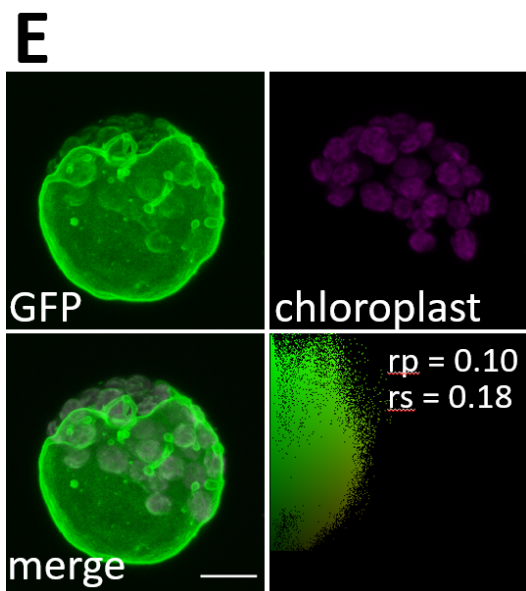


**Figure S10. Imaging of ACA8-11C-mGFP5 in various tissues and cell types.** mGFP5 expression patterns in 10-day old seedlings stably expressing *UBQ10::ACA8-11C-mGFP5* were obtained in the **(A, D)** root differentiation zone, **(B)** guard cells, **(C)** root elongation zone. mGFP5 expression does not colocalize with plasma membrane marker FM5-95. Short incubation time (30 minutes) with DND-99 stains the lumen of root cell vacuoles in **(D)**. **(E)** Maximum intensity projection showing tonoplast localization of ACA8-11C-mGFP5. 2D colocalization histograms with Pearson's (rp) or Spearman's (rs) correlation coefficients, suggest limited colocalization with chloroplasts. Scale bar = 5  $\mu$ m.

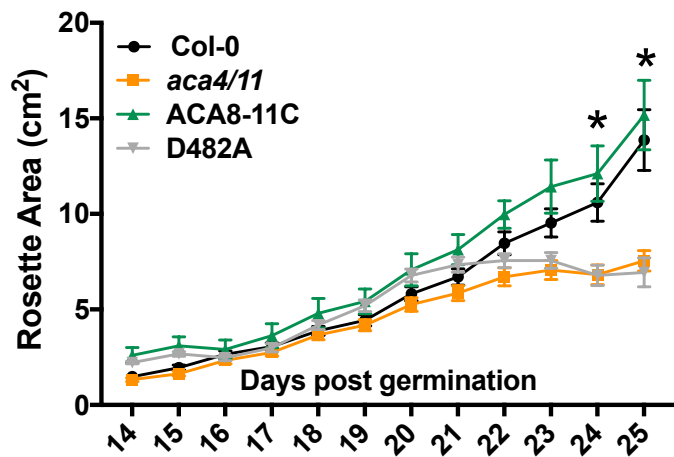


**Figure S11. ACA8-11C suppresses *aca4/11* rosette growth phenotype.** Time-course measurements of rosette area. Asterisks denote days when *aca4/11* and *aca4/11* + D482A rosette areas were significantly smaller than both Col-0 and *aca4/11* + ACA8-11C rosettes (One-way ANOVA; Tukey's HSD;  $p < 0.05$ ); data is presented as mean  $\pm$  s.e.m. and representative of  $n \geq 24$  rosettes. The experiment was performed 3 times with similar results.

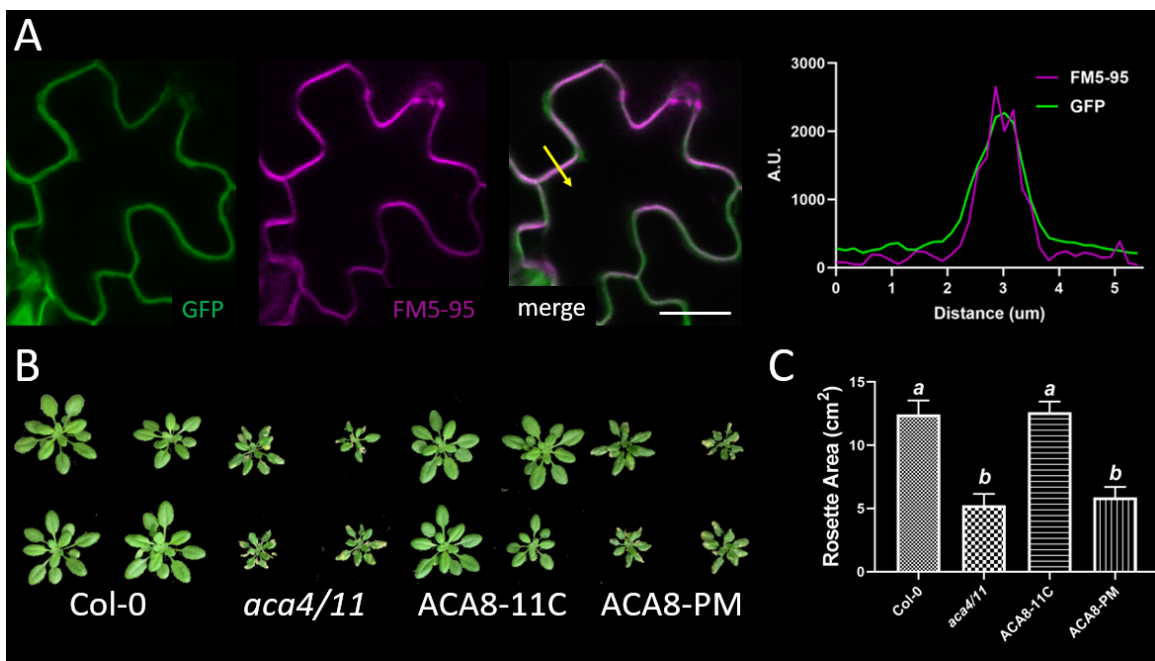


**Figure S12. Overexpression of ACA8 at the plasma membrane does not rescue the *aca4/11* lesion and dwarfism phenotypes.** Confocal micrograph and line profile of yellow arrow showing ACA8-GFP colocalization with the PM marker FM5-95 (A); scale bar = 10  $\mu\text{m}$ . Representative images of 25-day-old rosettes from Col-0, *aca4/11*, *aca4/11* + ACA8-11Cterm, and *aca4/11* + ACA8-PM (B). Rosette area measurements of 25-day-old plants (C). *aca4/11* plants overexpressing ACA8 at the plasma membrane (ACA8-PM) did not revert to wildtype size (One-way ANOVA; Tukey's HSD;  $p < 0.05$ ); data is presented as mean  $\pm$  s.e.m. and representative of  $n \geq 24$  rosettes; the experiment performed several times with similar results.

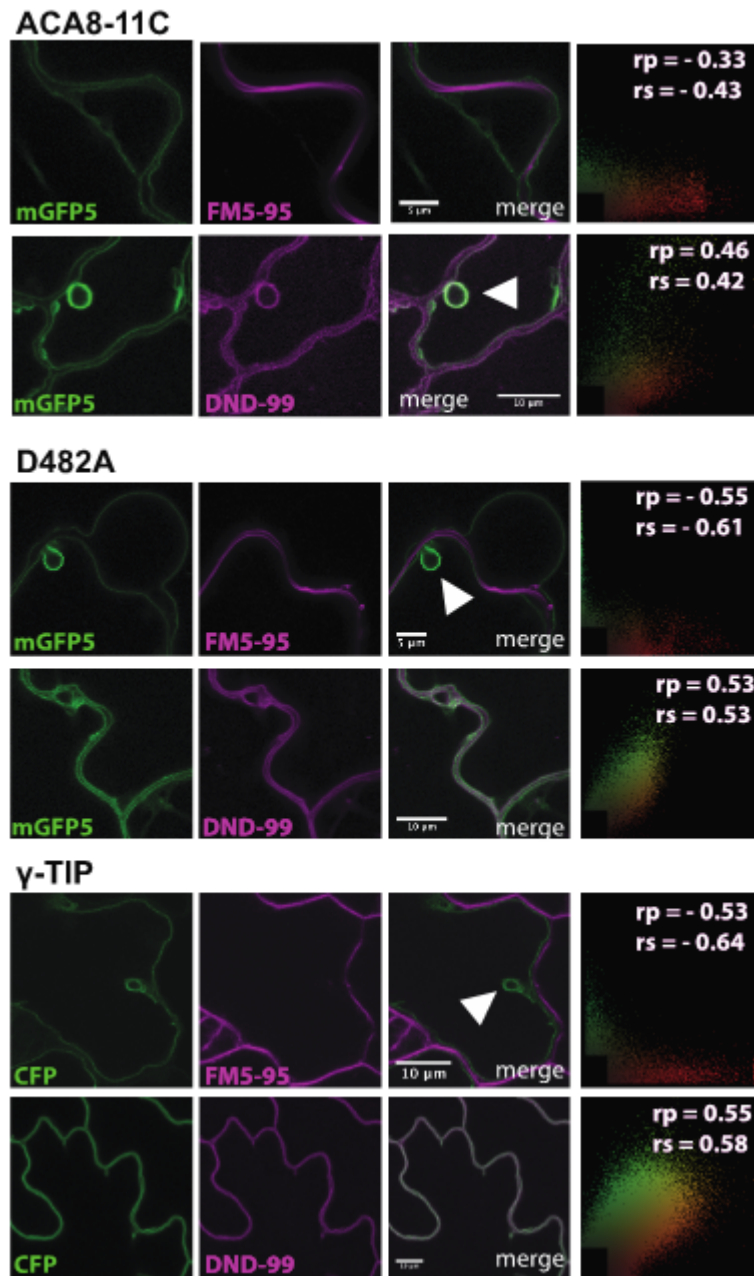


**Figure S13. The C-terminus of ACA11 localizes ACA8 to the tonoplast.** Confocal images of *aca4/11* cotyledons expressing *UBQ10::ACA8-11C-mGFP5* or *UBQ10::ACA8-D482A-11C* stained with either the tonoplast reporter Lysotracker Red-DND99 (DND99) or the plasma membrane staining dye FM5-95. Col-0 wildtype plants expressing 35S:: $\gamma$ -TIP-CFP was used as a tonoplast colocalization control 2D colocalization histograms indicate Pearson's (rp) or Spearman's (rs) correlation coefficients in top right corners. White arrows indicate the presence of tonoplast bulb structures. Representative of >10 images; scale bar = 10  $\mu$ m.

**Table S1.** qPCR primers used for this study.

Target	Sequence (5' to 3')	Direction	Length	Reference to flg22-responsiveness
<i>UBQ10</i>	CAC ACT CCA CTT GGT CTT GCG T TGG TCT TTC CGG TGA GAG TCT TCA	Forward Reverse	22 24	-
<i>CBP60g</i>	AAT AAC GAG GAG GAT GAG AAC G TCA GAC ACG GTA AGA AAC ATC G	Forward Reverse	22 22	Zheng <i>et al.</i> , 2015
<i>ICS1</i>	TTC CAG CAG AAG AAG CAA GG GAT CCC GAC TGC AAA TTC AC	Forward Reverse	20 20	Zheng <i>et al.</i> , 2015
<i>PHI1</i>	TTG GTT TAG ACG GGA TGG TG ACT CCA GTA CAA GCC GAT CC	Forward Reverse	20 20	Boudsocq <i>et al.</i> , 2010
<i>FLS2</i>	ACT CTC CTC CAG GGG CTA AGG AT AGC TAA CAG CTC TCC AGG GAT GG	Forward Reverse	23 23	-
<i>FRK1</i>	CGG TCA GAT TTC AAC AGT TGT C AAT AGC AGG TTG GCC TGT AAT C	Forward Reverse	22 22	Boudsocq <i>et al.</i> , 2010

\*All primers sequences were either derived from references paper or designed using the Web Tools available at [www.idtdna.com](http://www.idtdna.com). M. Boudsocq, *et al.*, Differential innate immune signalling via Ca(2+) sensor protein kinases. *Nature* **464**, 418–22 (2010); X.-Y. Zheng, *et al.*, Spatial and temporal regulation of biosynthesis of the plant immune signal salicylic acid. *Proc. Natl. Acad. Sci.* **112**, 9166–9173 (2015).

**Table S2.** Cloning primers and gBlock used for this study.

Target	Sequence (5' to 3')	Direction
<i>UBQ10pro</i>	532 - tac <b>GGTACC</b> GAGTCAGTAATAAACGGC	Forward
	533 - tac <b>CCATGGgtcgactattctaga</b> CTGTTAACAGAAAAACTCAG	Reverse
<i>ACA8ΔC</i>	525 - tac <b>TCTAGA</b> ATGACGAGTCTCTGAAGTCATGCCGTG	Forward
	526 - tac <b>gtcgac</b> CGCAATTACCAAGGAACCAACAATG	Reverse
<i>ACA8-11C</i>	571 - gagttttctgattaacagtctag <b>ATGACGAGTCTCTGAAGTC</b>	Forward
	572 - agctcggtaccgggtta <b>cttgcgtcatcgcttttagtc</b> GGCAGAGTCAGATGGACC	Reverse
<i>D482A_1</i>	633 - aatctgagttttctgattaacagtctag <b>ATGACGAGTCTCTGAAGTC</b>	Forward
	634 - <b>gttccagtttag</b> CGCTGCAAATAGTGGTGG	Reverse
<i>D482A_2</i>	635 - <b>actatttgca</b> cg <b>CTAAACTGGAACACTAACTC</b>	Forward
	636 - tccagtgaaaaggttctcccttactag <b>TCAGATCTACCATGTCGAC</b>	Reverse

**gBlock5 Sequence (5' > 3'):**

GGTCTATATAAtgttgagttccttgtaaattcgctcgACGACGAAACTAAACTGGAAGCAATG  
 GCTTATCTGTGTTGGCATCGGTGTTATCAGTTGGCCTCTGCTTGCGGG  
 AATGCATACCGGTTGAGTCTAACCGTCATCACGATGGCTATGAGCTGCTTCCT  
 TCTGGTCCATCTGACTCTGCCgtcgacatggtagatctgactagtagaaaggATATGAGACCTC  
 AGTTGGCCTTGCTTGGTCGGAAATGCATACCGGTTGAGTCTAACCGTCA  
 TCACGATGGCTATGAGCTGCTTCCTCTGGCCATCTGACTCTGCCgtcgacatggta  
 gatctgactagtagaaaggA

\*gBlock5 designed using NEB HiFi Assembly Tool (<https://nebuilder.neb.com/>)

**Movie S1 (separate file).** Time-lapse calcium imaging of a Col-0 rosette during 1  $\mu$ M flg22 treatment.

**Movie S2 (separate file).** Time-lapse calcium imaging of an *aca4/11* rosette during 1  $\mu$ M flg22 treatment.

**Movie S3 (separate file).** Time-lapse calcium imaging of a Col-0 cotyledon during 1  $\mu$ M flg22 treatment.

**Movie S4 (separate file).** Time-lapse calcium imaging of an *aca4/11* cotyledon during 1  $\mu$ M flg22 treatment.

**Movie S5 (separate file).** Time-lapse calcium imaging of an ACA8-11C cotyledon during 1  $\mu$ M flg22 treatment.